

## Article

# Insights into the Crustal Evolution and Tungsten Mineralization of the West Cathaysia Block: Constraints from the Inherited Zircons from the Mesozoic Dengfuxian and Paleozoic Tanghu Plutons, South China

Jingya Cao <sup>1,2,3</sup> , Youyue Lu <sup>1,\*</sup>, Lei Liu <sup>4,\*</sup>, Jianming Fu <sup>1</sup>, Guofeng Xu <sup>4</sup>, Qianhong Wu <sup>4</sup>, Shengxiong Yang <sup>2</sup>, Xiaofei Qiu <sup>1</sup> and Zunzun Zhang <sup>1</sup>

<sup>1</sup> Research Center for Petrogenesis and Mineralization of Granitoid Rocks, China Geological Survey, Wuhan 430205, China

<sup>2</sup> Southern Marine Science and Engineering Guangdong Laboratory (Guangzhou), Guangzhou 511458, China

<sup>3</sup> Department of Ocean Science, The Hong Kong University of Science & Technology, Hong Kong, China

<sup>4</sup> Key Laboratory of Metallogenic Prediction of Nonferrous Metals and Geological Environment Monitoring, Ministry of Education, Central South University, Changsha 410083, China

\* Correspondence: luyouyue@mail.ustc.edu.cn (Y.L.); liu01@ustc.edu.cn (L.L.)

**Abstract:** The formation and evolution of the ancient continental crust are crucial issues in solid-earth geology which are commonly associated with global tectonic events and the formation of economically valuable magmatic-hydrothermal ore deposits. The Cathaysia Block, one of the ancient continents in Southeast Asia, can be subdivided into two parts: the West Cathaysia Block and the East Cathaysia Block. Unlike the East Cathaysia Block, no Precambrian rocks are exposed in the West Cathaysia Block, constraining further understanding of the formation and evolution of this block. In this study, a total of four hundred and thirty-three zircon U-Pb dating analyses and two hundred and eighteen Lu-Hf isotopic analyses on zircon grains from the Jurassic Dengfuxian granites and Ordovician Tanghu granites, Nanling Range, were carried out. LA-ICP-MS zircon U-Pb dating yields mean average  $^{206}\text{Pb}/^{238}\text{U}$  ages of  $152.6 \pm 2.2$  Ma (MSWD = 1.6) and  $442.4 \pm 1.7$  Ma (MSWD = 3.8), which are regarded as the rock-forming age for the Jurassic Dengfuxian granites and Ordovician Tanghu granites, respectively. The  $^{207}\text{Pb}/^{206}\text{Pb}$  ages of the inherited zircons from the Jurassic Dengfuxian granites and Ordovician Tanghu granites range from 522 Ma to 3395 Ma, hosting two major peaks at the 0.9–1.0 Ga and 2.4–2.5 Ga. In contrast to the East Cathaysia Block, the West Cathaysia Block lacks the age peak of 1.8–1.9 Ga, indicating that the West Cathaysia Block was not influenced by the assembly of the Columbia supercontinent in the Paleo-Proterozoic. In combination with the Lu-Hf isotopes, we proposed that the crust evolution of the West Cathaysia Block in Archean is dominated by juvenile crustal growth events, and dominated by the crustal reworking since the Proterozoic. The long duration of crustal reworking in the West Cathaysia Block resulted in the enrichment of lithophile elements (e.g., W, Sn, Nb, and Ta) in the crust of that region. Therefore, the Jurassic granites in the Nanling Range, which are mainly derived from the partial melting of Proterozoic basement rocks, became associated with large-scale tungsten polymetallic mineralization.

**Keywords:** U-Pb ages; Lu-Hf isotopes; inherited zircons; crustal evolution; South China



**Citation:** Cao, J.; Lu, Y.; Liu, L.; Fu, J.; Xu, G.; Wu, Q.; Yang, S.; Qiu, X.; Zhang, Z. Insights into the Crustal Evolution and Tungsten Mineralization of the West Cathaysia Block: Constraints from the Inherited Zircons from the Mesozoic Dengfuxian and Paleozoic Tanghu Plutons, South China. *Minerals* **2023**, *13*, 550. <https://doi.org/10.3390/min13040550>

Academic Editor: Alexey V. Ivanov

Received: 31 January 2023

Revised: 6 April 2023

Accepted: 10 April 2023

Published: 13 April 2023



**Copyright:** © 2023 by the authors. Licensee MDPI, Basel, Switzerland. This article is an open access article distributed under the terms and conditions of the Creative Commons Attribution (CC BY) license (<https://creativecommons.org/licenses/by/4.0/>).

## 1. Introduction

Understanding crustal generation and reworking, essential for the formation and evolution of the global continental crust, commonly depends on the basement rocks of each continent. The nature of these rocks can provide key information, not only on the formation and evolution of the crust but also on the origin of polygenetic granites and related mineral deposits [1–8]. However, these rocks in some early Precambrian cratons might be overprinted and/or obscured, caused by the intensive thermo-tectonic events [9,10]. The

Cathaysia Block, one of the important parts of the South China Block, is well-known for its intensive polygenetic tectonic-magmatism and related rare metal mineralization [11–20]. To date, the Paleoproterozoic Badu Group exposed in the south-western Zhejiang province and north-western Fujian province are well accepted as the oldest rock unit in the Cathaysia Block [21–26]. Hence, the Precambrian crust evolution of the Cathaysia Block is poorly understood due to the absence of Archean rocks. Although no Archean rocks were found in the Cathaysia Block, abundant Archean and even Hadean ages of the inherited zircon grains in igneous and detrital zircon grains in sedimentary rocks and/or river sediments were reported [4,22,23,26–29]. Therefore, several geologists argued that the Archean basement rocks of “Cathaysia old continent” might exist in the Cathaysia Block, however, they might be broken up into several microplates and/or reworked by the subsequent tectonic-magmatic events [9,30]. Further studies indicated that the Cathaysia Block can be subdivided into the West Cathaysia Block and East Cathaysia Block, which consist of the Yunkai-Nanling and Wuyi terranes, respectively [4,11]. The Precambrian rocks are well exposed in the East Cathaysia Block, including the Paleo-Proterozoic metasedimentary rocks and granites [21–23,31]. Conversely, rare Precambrian rocks are identified in the West Cathaysia Block, constraining the understanding of the formation and evolution of the Precambrian crust of the West Cathaysia Block.

It is currently known that granitic rocks not only play an extremely important role in the evolution of the Earth’s crust [32–34], they also are commonly accompanied by migration and/or enrichment of elements and the formation of intense tungsten polymetallic mineralization [34,35]. The inherited zircons from the granites, which are commonly derived by partial melting of the deep crustal rocks, will elucidate the ages and source of these deep crust basement rocks and might provide a new perspective for geologists to unravel the missing geological records of the formation and evolution of the continental crust [36–39]. Nanling range is one of the important tungsten–tin polymetallic ore belts in South China and a world-famous tungsten mineralization province, hosting a series of large to super large tungsten deposits, e.g., Shizhuyuan, Xihuashan, Taoxikeng, Xiangdong, and Yaogangxian tungsten–tin deposits. In addition, these deposits are genetically linked to the granitic rocks both in time and space. Therefore, LA-ICP-MS U-Pb dating and LA-MC-ICPMS Lu-Hf isotopic analyses were carried out on these inherited zircons from the Mesozoic Dengfuxian and Paleozoic Tanghu plutons, Nanling Range, aiming to provide some insights into the generation and reworking history, and the relationship between the crust evolution and tungsten polymetallic mineralization of the West Cathaysia Block.

## 2. Regional Geology

The South China Block (SCB), composed of the Yangtze Block and the Cathaysia Block, is one of the largest Precambrian blocks in East Asia and might be formed by the amalgamation of these two blocks at ca. 820 Ma [12]. It was surrounded by the Qinling-Dabei orogenic belt to the north, the Songpan-Garze orogenic to the northwest, and Sibumasu-Indochina orogenic belt to the southwest (Figure 1a). Two blocks were proposed to be bounded by the Qinzhou-Hangzhou Belt, which starts from Hangzhou Bay to the northeast and Qinzhou Bay to the southwest (Figure 1b). The Yangtze Block, located at the northwest SCB, hosts a series of Mesoproterozoic-Archean igneous rocks, e.g., Kongling Group, Dongling Group, Douling Group, and Cuoque Group [40–45]. The Kongling Group, commonly regarded as the oldest exposed rock unit in the Yangtze Block, contains the Archean tonalite-trondhjemite-granodiorite (TTG) gneiss with ages of 3.2–3.3 Ga [41–43]. In addition, two-stage depleted mantle Hf model ages of zircon grains in the TTG gneiss show a significant peak at 3.3–3.5 Ga. Therefore, it is well accepted that an Archean basement might exist in the Yangtze Block [41–43]. Meanwhile, the Neoproterozoic igneous rocks are dominated by the arc-related basic and granitic rocks (820–850 Ma) which are mainly distributed in the margin area of the Yangtze Block, especially in the Jiangnan Orogen [46–49]. It is proposed that the Neoproterozoic oceanic subduction and/or arc-continent collision event might occur around the margin area of the Yangtze Block, which

might cause the collision between the Yangtze and Cathaysia blocks [12,24,50,51]. The Mesozoic granodiorite and granites in the Yangtze Block, mainly emplaced in Late-Jurassic and Early-Cretaceous and related to the regional Cu-Au-W polymetallic mineralization, are involved in the Pacific subduction event toward the South China Block, for example, the Cu-Au deposits of the Tongling ore cluster and the Chating ore cluster [52–57].

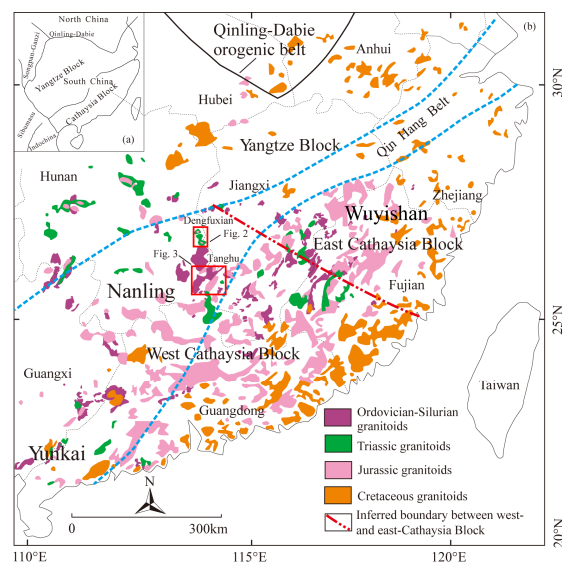


**Figure 1.** The sketch tectonic location of the South China Block (a) and the Geological sketch map of the South China Block (b), modified from [58]. The inferred boundary between the West and East Cathaysia Block is modified from [4]. The red box refers to the study regions, whereas the area between the blue dashed lines refers to the Qian-Hang Belt of SE China. The grey dashed lines refer to the provincial boundaries.

Unlike the Yangtze Block, the Archean basement rocks are absent in the Cathaysia Block, however, a series of Archean-Hadean detrital zircon ages were reported, indicating that the Archean basement and/or Hadean fragments might exist in the Cathaysia Block [4,21,26–29]. The Precambrian rocks exposed in this block are mostly distributed between the NE-trending Qin-Hang Belt and Zhenghe-Dapu fault (Figure 1b), e.g., the Paleoproterozoic Badu Group and Mesoproterozoic Longquan Group in the Wuyishan area, the East Cathaysia Block, and Neoproterozoic Sibao Group in the Nanling Range, and the West Cathaysia Block. The Badu Group mainly comprises the mica schists, gneisses, and migmatites, which were mainly formed at ca. 2.5 Ga and subsequently reworked in ca. 1.8 Ga and 250–230 Ma, respectively [21,59]. The Longquan Group is mainly composed of mica-quartz schist, epidote amphibolite, actinolite schist, and fine-grained biotite gneiss, showing that the protoliths of mafic volcanic rocks and pelitic-arenaceous-calcareous sedimentary rocks experienced greenschist to low amphibolite facies metamorphism [21]. Sm-Nd isotopic dating suggests that rocks of the Longquan Group might be formed at 1.4–1.0 Ga, however, detailed age data are lacking [59,60]. The Sibao Group, mainly composed of epimetamorphic shale and volcanoclastic rocks, metamorphosed basalts, spilite, and keratophyre, might have been formed at ca. 830 Ma [61]. The Paleozoic strata are widespread in the Cathaysia Block, including a series of marine to continental sedimentary rocks. However, they have experienced various degrees of deformation due to the following tectonic events.

The oldest igneous rocks, mainly S- and/or A-type granites, were distributed in the Wuyishan area, Eastern Cathaysia Block, with ages of 1.8–1.9 Ga [22,23]. However, rare Paleoproterozoic igneous rocks were identified in the Nanling-Yunkai region. The igneous rocks in the Cathaysia Block are dominated by the Mesozoic granitoid with few Middle Paleozoic granitoids (Figure 1b). The Middle Paleozoic granitoids, related to uranium mineralization, are mainly located in the Nanling Range with peak ages of 444–419 Ma [62].

The Mesozoic granitoids, especially Jurassic granitoids, are widespread in the Cathaysia Block and are associated with the regional W-Sn polymetallic mineralization. These Jurassic granites, mainly emplaced at 165–150 Ma, are related to the intense magmatic magmatism which was derived by the partial melting of the Proterozoic basement rocks of the Cathaysia Block and triggered by the Pacific subduction event [17].

### 3. Sampling and Analytical Methods

#### 3.1. Sampling and Description

Two fresh samples were collected from the Nanling Range, West Cathaysia Block, including a two-mica monzonitic granite from the Dengfuxian composite pluton (Figure 2a) and a biotite monzonitic granite from the Tanghu pluton (Figure 3a). The Dengfuxian composite pluton, located in Eastern Hunan, is composed of the Triassic biotite monzonitic granite and Jurassic two-mica monzonitic granite, with ages of  $225.7 \pm 1.6$  Ma and  $151.1 \pm 1.5$  Ma, respectively [63,64]. A two-mica monzonitic granite sample was collected from the Dengfuxian composite pluton, and the sampling location was represented in Figure 2a. In addition, the Jurassic granites, genetically related to the large-scale tungsten mineralization, belong to the S-type granite and originated from the partial melting of the Precambrian basement rocks of the Cathaysia Block [65,66]. The Jurassic two-mica monzonitic granites are mostly grey with a fine-grained texture, consisting of K-feldspar (~25%), plagioclase (~20%), quartz (~35%), muscovite (~12%), and biotite (~8%) (Figure 2b,c). These granites also contain accessory minerals of apatite, zircon, and titanite.

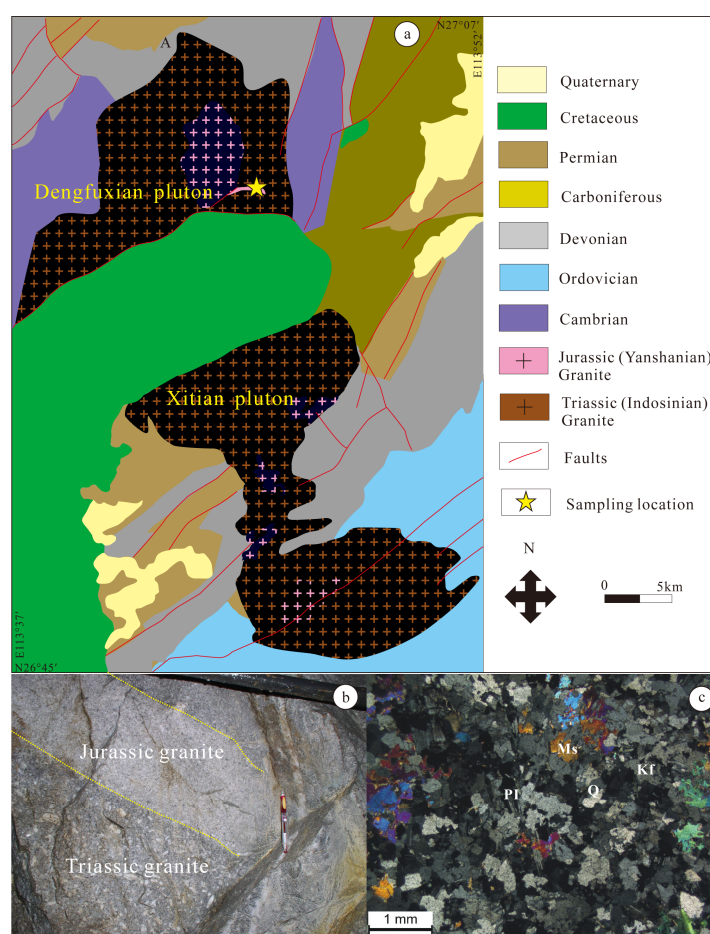


**Figure 2.** Geological sketch map of the Xitian and Dengfuxian plutons (a), modified from [67]; Outcrop (b) and orthogonal polarizing micrograph (c) of the Dengfuxian Jurassic granite. The location of Figure 2a has been shown in Figure 1b.

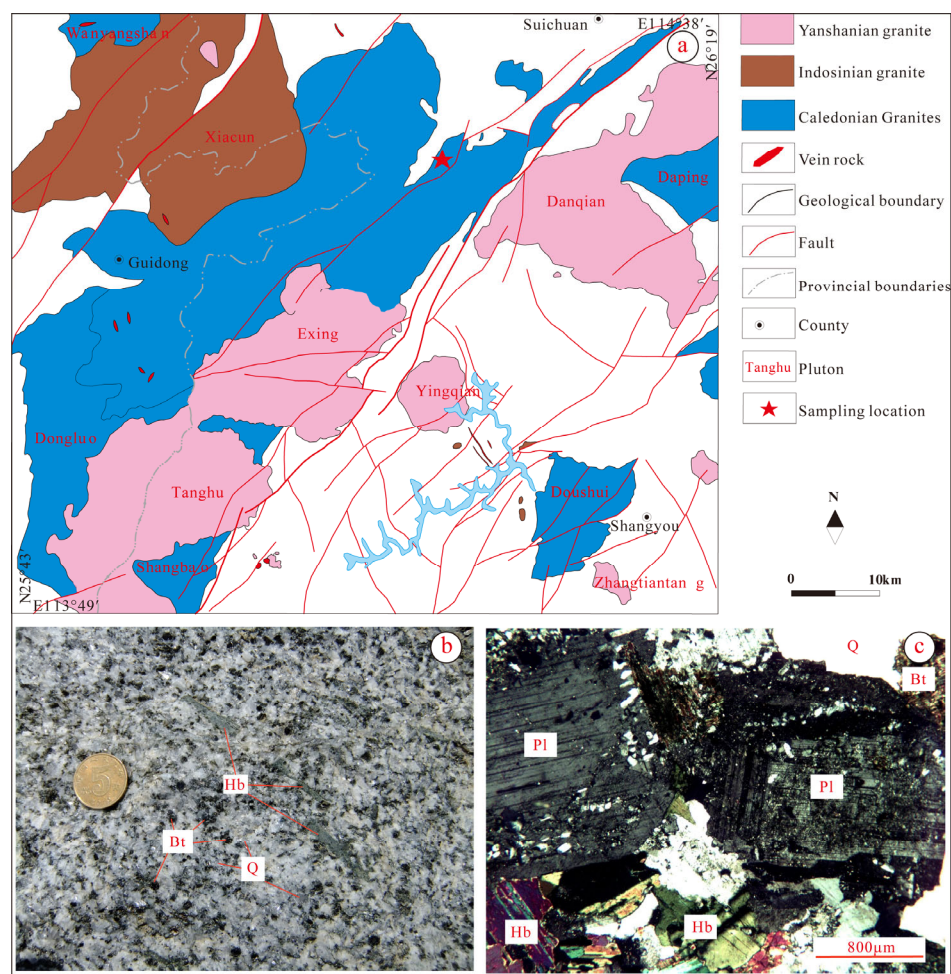


**Figure 3.** Geological sketch map of the north Zhuguangshan area (a); Outcrop (b) and orthogonol polarizing micrograph (c) of the Tanghu granite. The location of Figure 3a has been shown in Figure 1b.

The Tanghu pluton, part of the Zhuguangshan composite pluton which is composed of Ordovician, Triassic, and Jurassic granites, is located at the junction region between Jiangxi and Guangdong [68]. The Tanghu pluton is composed of biotite monzonitic granite and granodiorite with a precise U-Pb age of ca. 440 Ma, indicating that the formation of these Ordovician granites has a close link with the Caledonian orogeny in South China [68]. A biotite monzonitic granite sample was collected from the Tanghu pluton, and the sampling location was shown in Figure 3a. The Tanghu biotite monzonitic granite is mostly grey with a porphyritic-like texture (Figure 3b). Phenocrysts are mainly composed of subhedral tabular plagioclase, which commonly hosts a zonary structure (Figure 3c). Mineral assemblages are composed of K-feldspar (15%~25%), plagioclase (35%~45%), quartz (20%~25%), and biotite (5%), with accessory minerals of magnetite, apatite, zircon, and titanite.

### 3.2. Analytical Methods

#### 3.2.1. Selection and CL Imaging of Zircon

Based on the conventional magnetic and heavy liquid techniques, zircon grains were first separated from the Dengfuxian Jurassic granites (sample no. 0326–2s2) and Tanghu Ordovician granites (sample no. 13D40). Second, they were handpicked under a binocular microscope. Third, they were mounted into epoxy resin blocks and polished to obtain flat surfaces. Before the LA-ICP-MS U-Pb dating analyses, these zircon grains were photographed and observed under an electron microscope to avoid inclusions and fractures in these grains. Finally, these zircon grains were photographed through a scanning electron mi-

croscope (TESCAN MIRA 3 LMH FE-SEM, TESCAN, Brno, Czech Republic) at the Sample Solution Analytical Technology Co., Ltd, Wuhan, China, to get the Cathodoluminescence (CL) images.

### 3.2.2. LA-ICP-MS Zircon U-Pb Dating

Ninety-two and three hundred and forty-two U-Pb dating and trace element analyses of zircons were collectively conducted by LA-ICP-MS at the Laboratory of Isotope Geochemistry, Wuhan Center of China Geological Survey for the Dengfuxian and Tanghu granites, respectively. The LA-ICP-MS were assembled by an icapQ ICP-MS instrument and a resolution laser ablation system. The former was used to obtain ion-signal intensities, whereas the latter was used to denude the samples. The helium and argon were used as the carrier gas and the make-up gas, respectively, which were optimized by ablating NIST SRM 610 to obtain maximum signal intensity for  $^{238}\text{U}$  and to keep low ThO/Th (0.01%–0.03%) and  $\text{Ba}^{2+}/\text{Ba}^{+}$  ratios (0.02%–0.03%) to reduce the matrix-induced interferences. Average intensities of  $^{202}\text{Hg}$ ,  $^{204}(\text{Pb} + \text{Hg})$ ,  $^{206}\text{Pb}$ ,  $^{207}\text{Pb}$ , and  $^{208}\text{Pb}$  of the gas blank were lower than 50 cps at a sensitivity of  $0.4 \times 10^6$  cps  $^{238}\text{U}$ . In this analysis, a spot size of 29  $\mu\text{m}$  and an energy density of 4 J/cm<sup>2</sup> were applied. The detailed procedure was as follows: (1) Each analysis contained approximately 15 s of background acquisition (gas blank) followed by 45 s of data acquisition; (2) The standard zircon 91500 was analyzed twice in every eight analyses of the unknowns. In addition, the U-Th-Pb isotopic ratios were calibrated relative to this standard zircon 91500 whose age is ca.  $1064.5 \pm 0.6$  Ma [69]. Common Pb correcting was followed by using the model proposed by [70]. Further data processing for zircon U-Pb dating and trace elements were performed by the software ICPMSDataCal 10.7 [71], while concordia diagrams and age calculations were obtained by using the software Isoplot v.3.0 [72].

### 3.2.3. LA-MC-ICP-MS Zircon Lu-Hf Isotope Analysis

Ninety-two and one hundred and twenty-seven in situ Lu-Hf isotope ratio analyses of zircons were conducted using a Neptune Plus MC-ICP-MS combined with a RESolution laser ablation system at the Laboratory of Isotope Geochemistry, Wuhan Center of China Geological Survey for the Dengfuxian and Tanghu granites, respectively. Helium and argon were used as the carrier gases during the process. Masses of  $^{171}\text{Yb}$ ,  $^{173}\text{Yb}$ ,  $^{175}\text{Lu}$ ,  $^{176}(\text{Hf} + \text{Yb} + \text{Lu})$ ,  $^{177}\text{Hf}$ ,  $^{178}\text{Hf}$ ,  $^{179}\text{Hf}$ , and  $^{180}\text{Hf}$  were measured by a 60 s of ablation signal acquisition and followed by 30 s of wash time. The size of the laser spot diameter and the energy density were set by 43  $\mu\text{m}$  and 6 J/cm<sup>2</sup>, respectively. The detailed correcting process of the interference of  $^{176}\text{Yb}/^{176}\text{Hf}$  and  $^{176}\text{Yb}/^{177}\text{Hf}$  were following the methods proposed by Thirlwall et al. (2004) [73]. The  $^{176}\text{Lu}/^{177}\text{Hf}$  ratio was calculated by using the recommended  $^{176}\text{Lu}/^{175}\text{Lu} = 0.02656$  [74]. Offline data processing was performed using the software ICPMSDataCal 10.7 [71]. Reference standard zircons 91500 and Pl sovice were analyzed as “unknowns” to control the reproducibility and instrument stability. In this analysis, the  $^{176}\text{Hf}/^{177}\text{Hf}$  of standard zircons 91500 and Pl sovice were  $0.282297 \pm 0.000002$  (MSWD = 1.5,  $n = 126$ ) and  $0.282479 \pm 0.000001$  (MSWD = 1.4,  $n = 134$ ), respectively, and both agree with the reference values of  $0.282307 \pm 0.000031$  [75] and  $0.282482 \pm 0.000013$  [76], respectively. The decay constant value  $^{176}\text{Lu}$  was  $1.867 \times 10^{-11} \text{ a}^{-1}$  for [77], while the  $\epsilon_{\text{Hf}}(t)$  values were calculated by using the present-day chondritic ratios of  $^{176}\text{Hf}/^{177}\text{Hf} = 0.282785$  and  $^{176}\text{Lu}/^{177}\text{Hf} = 0.0336$  [78]. The crustal model age ( $T_{\text{DMC}}$ ) calculation was assuming that the parental magma was produced from the average continental crust ( $^{176}\text{Lu}/^{177}\text{Hf} = 0.015$ ) that was primarily derived from the depleted mantle [79]. A detailed analytical procedure was described by [75].

## 4. Results

### 4.1. Zircon Characteristics

Zircon grains from the Dengfuxian granites (0326–2s2) are mostly characterized by regular to irregular prisms with light yellow to colorless, a length of 100–250  $\mu\text{m}$ , a width of

80–120  $\mu\text{m}$  and aspect ratios of 3:1 to 1:1. Most of these zircon grains exhibit a clear zoning structure with no cores, however, some zircon grains show a rim-core structure (Figure 4a). These zircon grains with a rim-core structure contain a clear boundary between the rim and core with a zoning structure for the rims and a weak zonation for the cores, respectively. In addition, most of the cores are characterized by bright fluorescence under the CL images.

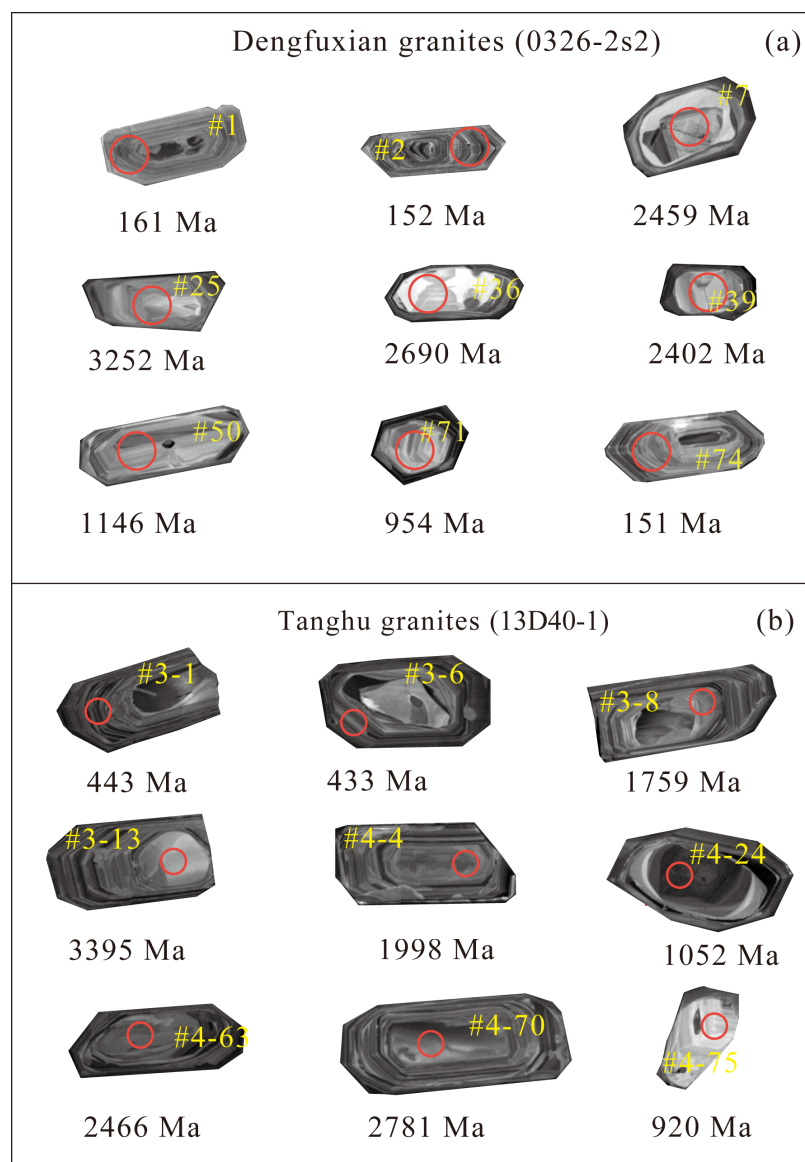


**Figure 4.** Cathodoluminescence (CL) images of zircons from the Dengfuxian (a) and Tanghu granites (b). The red circle is the location for the LA-ICP-MS dating. The red circle diameter, marked on zircons, is ca. 29  $\mu\text{m}$ . The numbers under the zircon grains represent the U-Pb ages of the corresponding zircon. The selected ages in this study followed the procedure that the young ages (lower than 1000 Ma) and old ages (higher than 1000 Ma) used  $^{206}\text{Pb}/^{238}\text{U}$  ages and  $^{207}\text{Pb}/^{206}\text{Pb}$  ages, respectively.

Zircon grains from the Tanghu granites (13D40) are mostly stubby prismatic with light yellow to colorless, a length of 100–400  $\mu\text{m}$ , a width of 100–200  $\mu\text{m}$ , and aspect ratios of 4:1 to 1:1. Most of these zircon grains exhibit a rim-core structure with a clear zoning structure for the rims and a weak zoning structure for the cores in the CL images (Figure 4b). In general, the cores show different features to the Dengfuxian zircon grains, since the Tanghu zircon grains mainly show a dark fluorescence under the CL images.

#### 4.2. Zircon U-Pb Isotopic Ages

Ninety-two U-Pb dating analyses were carried out on ninety-two zircon grains from the Dengfuxian granites (0326–2s2). These zircon grains from the Dengfuxian granites have variable U and Th contents of 18–1294 ppm and 27–3320 ppm, respectively (Table S1). The corresponding Th/U ratios range from 0.03 to 1.60 (mean = 0.59), however, most of them are over 0.1, suggesting a magmatic origin for most of these zircon grains (Figure 5) [80]. After rejecting a small number of analyses (concordance < 90%), the isotopic ages vary from 137 to 3252 Ma, hosting five major peaks at 150–160 Ma, 900–1000 Ma, 1100–1200 Ma, 1500–1600 Ma and 2300–2500 Ma. In addition, these zircon grains are mostly plotted on or near the concordant curve and can be subdivided into five populations which have ages of  $152.6 \pm 2.2$  Ma (MSWD = 1.6),  $966 \pm 12$  Ma (MSWD = 1.2),  $1115 \pm 23$  Ma (MSWD = 1.7),  $1558 \pm 76$  Ma (MSWD = 3.2) and  $2382 \pm 72$  Ma (MSWD = 1.4), respectively (Figure 6). These prismatic zircon grains with an age of  $152.6 \pm 2.2$  Ma, which is the same as the previously reported ages, are regarded to be formed during the emplacement of the Jurassic Dengfuxian granites.

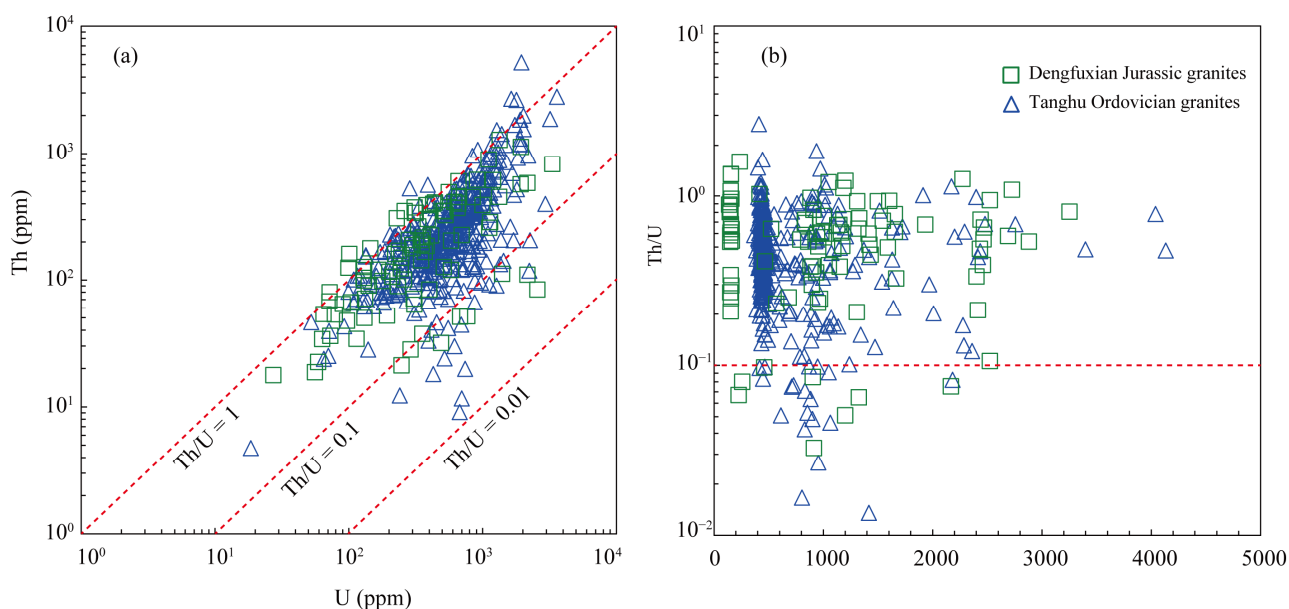


**Figure 5.** U versus Th (a) and age versus Th/U diagrams (b) of zircons from the Dengfuxian and Tanghu granites.

A total of three hundred and thirty-two zircon U-Pb dating analyses were carried out on three hundred and thirty-two zircon grains from the Tanghu granites (13D40-1). The U and Th contents for the zircon grains from the Tanghu granites were 19–3600 ppm and 5–5214 ppm, respectively (Table S1), with corresponding Th/U ratios of 0.01–2.67 (mean = 0.48), indicating a magmatic origin for most of these zircon grains (Figure 5) [80] (Table S1). After rejecting a small number of analyses (concordance < 90%), the isotopic ages vary from 367 Ma to 3395 Ma. Three major peaks at 400–500 Ma, 800–900 Ma, and 1000–1100 Ma were identified. In addition, these zircon grains are mostly plotted on or near the concordant curve (Figure 7a), yielding weighted mean ages of  $442.4 \pm 1.7$  Ma (MSWD = 3.8),  $896.2 \pm 8.8$  Ma (MSWD = 0.31) and  $1043 \pm 18$  Ma (MSWD = 2.5), respectively (Figure 7b,d). These prismatic zircon grains with an age of  $442.4 \pm 1.7$  Ma, which is the same as the previously reported ages, are regarded to be formed during the emplacement of the Tanghu Ordovician granites.

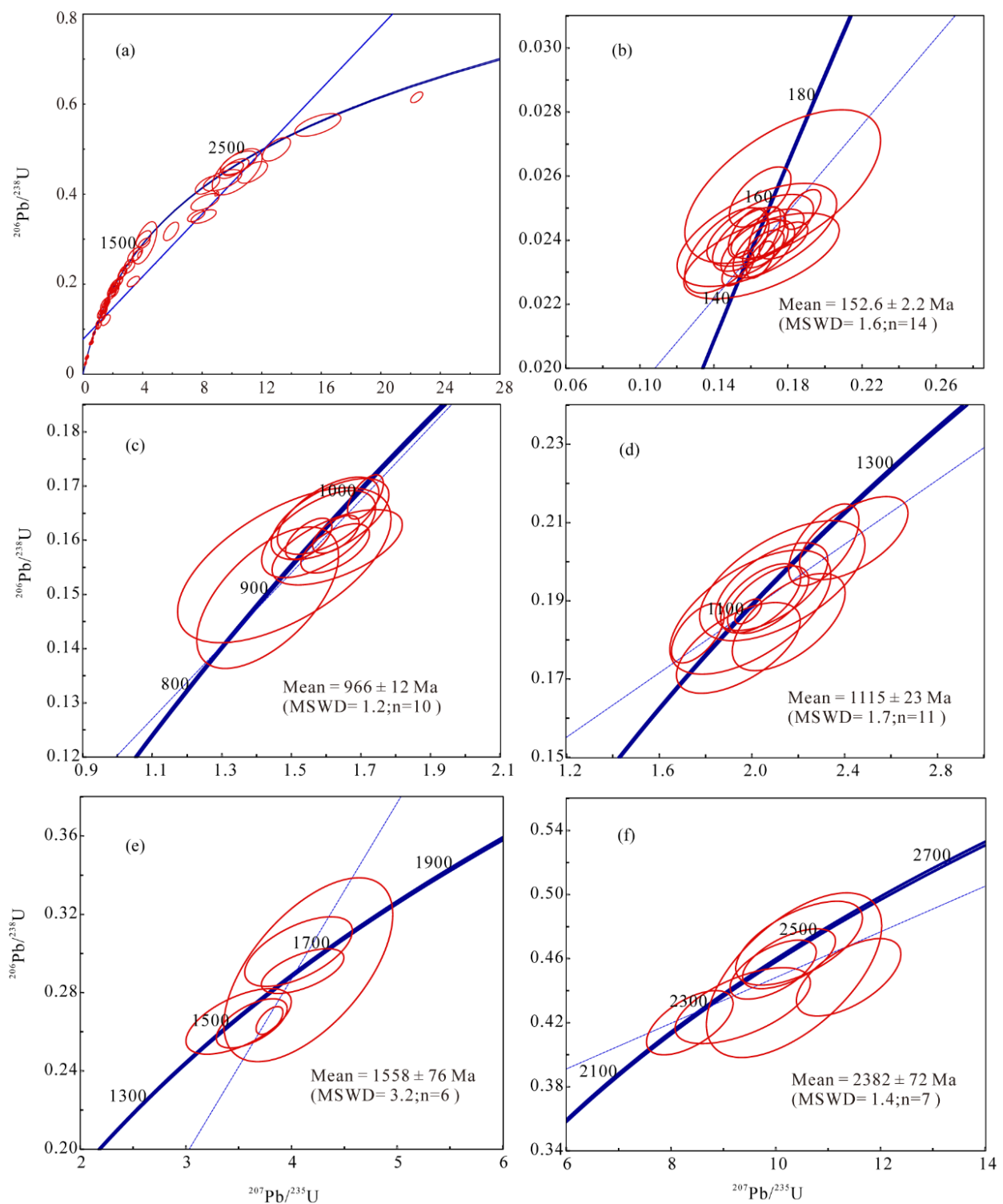


**Figure 6.** Concordia plots of zircon dating results for the Dengfuxian granites. (a) shows concordia plot of the whole data; (b,c) show concordia plot and mean average ages of Jurassic and Neoproterozoic, respectively. (d,e) show concordia plot and mean average ages of Mesoproterozoic zircons of ca. 1115 Ma and 1558 Ma, respectively; (f) show concordia plot and mean average age of Paleoproterozoic zircons. The red circle, blue solid lines and blue dashed lines represent the radius error for a single spot, concordant curve and unconcordant curve, respectively.

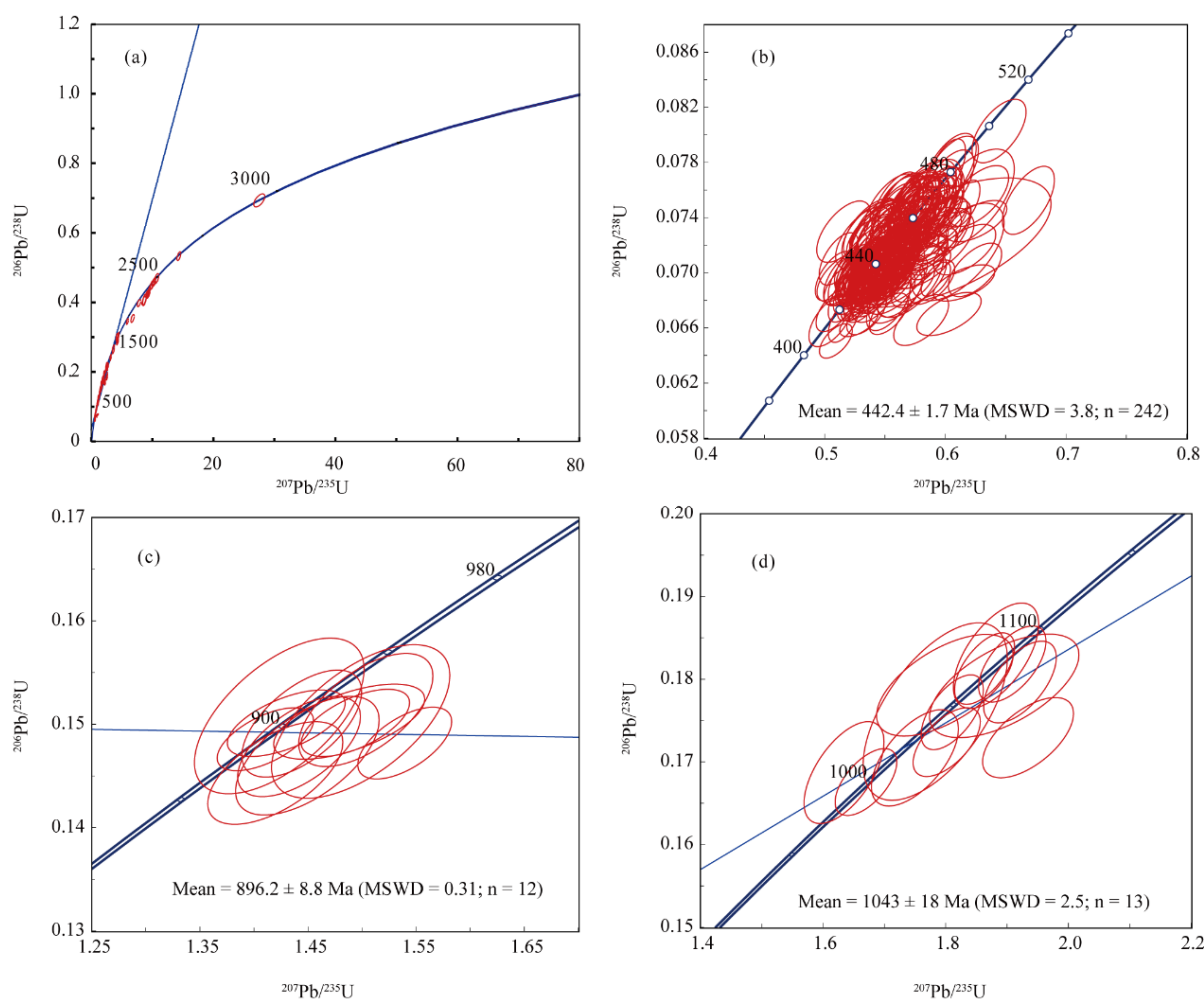


**Figure 7.** Concordia plots of zircon dating results for the Tanghu granites. (a) shows concordia plot of the whole data; (b–d) show concordia plot and mean average ages of Ordovician, Neoproterozoic and Mesoproterozoic zircons, respectively. The red circle, blue solid lines and blue dashed lines represent the radius error for a single spot, concordant curve and unconcordant curve, respectively.

#### 4.3. Zircon Lu-Hf Isotopes

Ninety-two Lu-Hf isotopic analyses were carried out on these zircon grains from the Dengfuxian granites (0326-2s2) which have been analyzed by U-Pb dating, and the results are represented in Table S2. In general, these zircon grains have variable  $^{176}\text{Hf}/^{177}\text{Hf}$  ratios of 0.28087–0.28256 with corresponding  $\varepsilon_{\text{Hf}}(t)$  values of −12.9 to 10.8 and crustal model ages ( $T_{\text{DMC}}$ ) of 1081–3583 Ma, respectively (Figures 8 and 9). Based on age populations of 150–160 Ma, 900–1000 Ma, 1100–1200 Ma, 1500–1600 Ma, and 2300–2500 Ma, they have  $\varepsilon_{\text{Hf}}(t)$  values of −11.3 to −5.8, −10.9 to 10.8, −12.9 to 10.5, −11.6 to 9.1, and −10.0 to 8.9 Ma, respectively. Their corresponding  $T_{\text{DMC}}$  ages are 1572–1918 Ma, 1081–2336 Ma, 1301–2779 Ma, 1615–3055 Ma, and 2602–3583 Ma, respectively.

One hundred and twenty-eight zircon Lu-Hf isotopic analyses were carried out on these zircon grains from the Tanghu granites (13D40-1) which have been analyzed by U-Pb dating, and the results are represented in Table S2. These zircon grains also have variable  $^{176}\text{Hf}/^{177}\text{Hf}$  ratios of 0.280223–0.282509 with corresponding  $\varepsilon_{\text{Hf}}(t)$  values of −35.2 to 13.8 and crustal model ages ( $T_{\text{DMC}}$ ) of 1306–4234 Ma, respectively (Figures 8 and 9). Based on age populations of 400–500 Ma, 800–900 Ma, and 1000–1100 Ma, they have  $\varepsilon_{\text{Hf}}(t)$  values of −10.1 to 0.06, −6.8 to 4.02, and −35.2 to 10.5, respectively. Their corresponding  $T_{\text{DMC}}$  ages range from 1431 to 2060 Ma, 1596 to 2189 Ma, and 1494 to 4061 Ma, respectively.

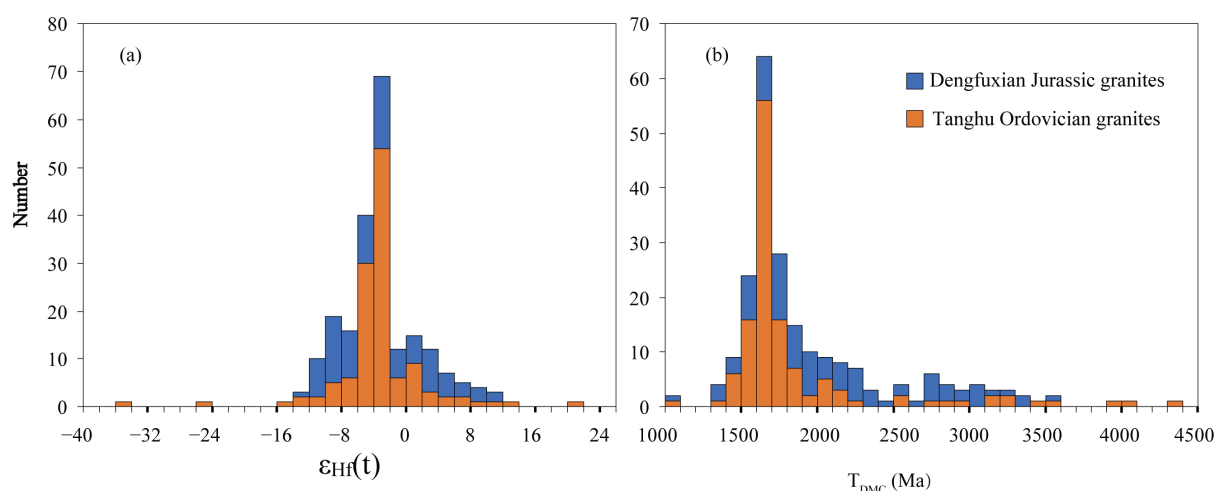


**Figure 8.** Histograms of zircon  $\epsilon_{\text{Hf}}(t)$  values (a) and Hf model ages ( $T_{\text{DMC}}$ ) (b) for the Dengfuxian and Tanghu granites.

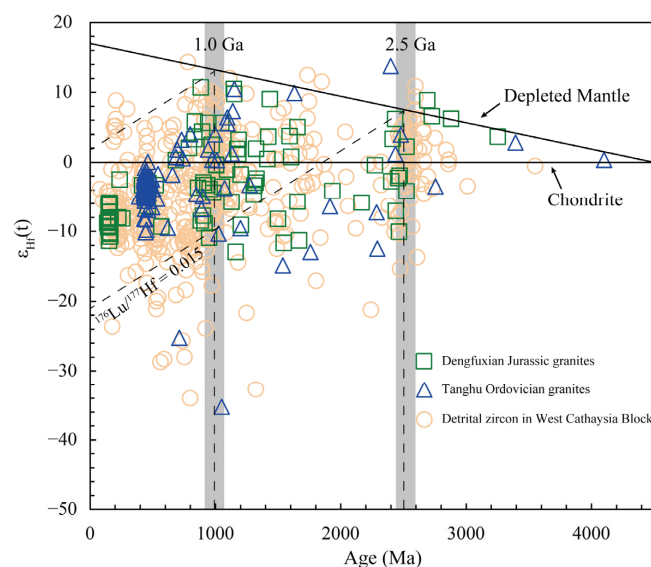


**Figure 9.** Zircon  $\epsilon_{\text{Hf}}(t)$  values versus U-Pb ages diagram. The data of the detrital zircons in the west Cathaysia Block are from [4,29,81,82], respectively.

## 5. Discussion

### 5.1. Precambrian Crust Evolutionary History of the West Cathaysia Block

#### 5.1.1. Archean (4000~2500 Ma)

Although no Archean rocks were exposed in the Cathaysia Block, geologists tend to believe that an Archean basement might be unexposed, although limited information on the Archean rocks was identified in the Cathaysia Block [9,23,30]. Recently, more and more geologists regarded that the Neo- and Meso-Archean (3200~2500 Ma) might be one of the key crustal generation periods of the Cathaysia Block since plentiful detrital zircon grains have an apparent age peak at ca. 2500 Ma in both the East and West Cathaysia Blocks (Figure 10) [10,15,28]. In addition, most of these zircon grains have positive  $\epsilon_{\text{Hf}}(t)$  values, indicating a mantle origin for the magma from which these zircons crystallized (Figure 9). Meanwhile, the difference between the zircon Hf model ages and the U-Pb ages, defined as the crustal incubation time [83,84], also have a cluster at ca. 2500 Ma, unraveling that the juvenile materials were involved in these zircons (Figure 11). In this study, both the Dengfuxian and Tanghu granites contain Neo- and Meso-Archean zircons with ages over 2500 Ma, positive  $\epsilon_{\text{Hf}}(t)$  values, and the consistent Hf model ages, further supporting

the perspective of a juvenile crust growth event for the West Cathaysia Block during the Neo- and Meso-Archean. However, it's worth noting that a considerable amount of Neo- and Meso-Archean detrital zircon grains have negative  $\varepsilon_{\text{Hf}}(t)$  values and Hf model ages of 2600–3600 Ma, signifying that crustal reworking is also a crucial aspect of the West Cathaysia Block crust evolution (Figure 9).

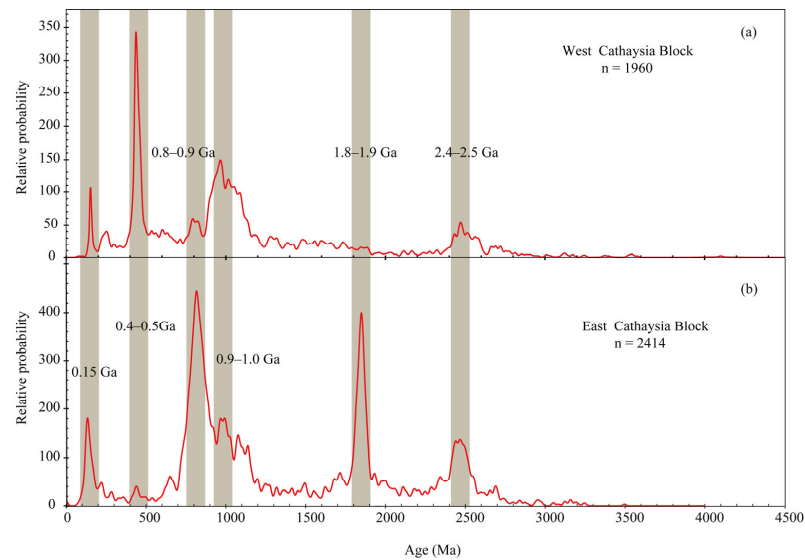


**Figure 10.** Relative probability density plots of detrital and inherited zircons from rocks of the WestCathaysia Block (a) and the East Cathaysia Block (b). In addition to the data in this study, the data of the West Cathaysia Block are from [4,11,28,29,81,82,85], respectively. The data of the East Cathaysia Block are from [22,25,31], respectively.

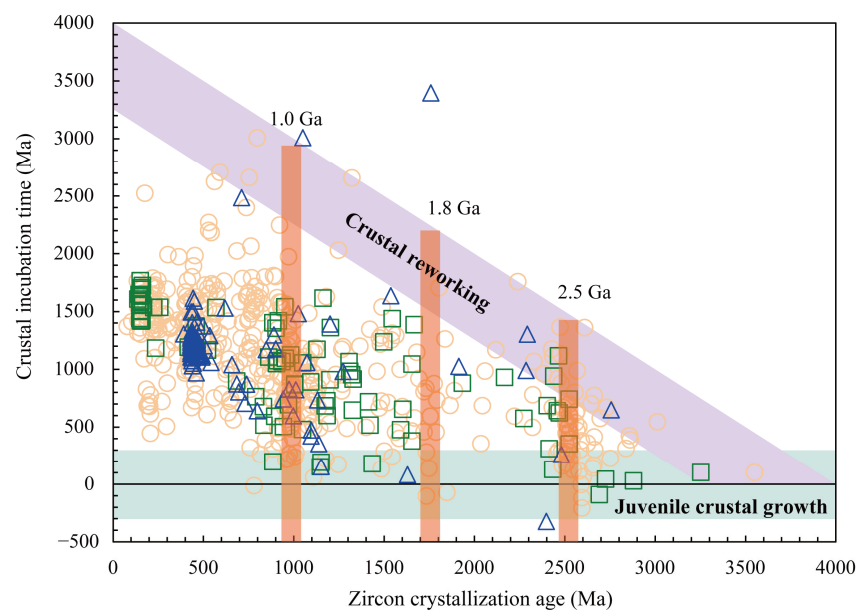


**Figure 11.** The plot of crustal incubation time versus crystallization ages of the detrital and inherited zircons from the (meta)sedimentary rocks in the Cathaysia Block. Crustal incubation time is defined by the difference between the zircon Hf model age and U–Pb crystallization age [83,84]. The data of the detrital zircons in the West Cathaysia Block are from [4,29,81,82], respectively. Green square, blue triangle and buff circle in this figure represent the inherited zircons from the Dengfuxian Jurassic granites, Tanghu Ordovician granites, and meta-sediments of the West Cathaysia Block, respectively.

The Paleoproterozoic crustal evolution of the West Cathaysia Block (4000–3200 Ma) is poorly understood since rare detrital zircon grains were identified in comparison to the Neo- and Meso-Archean. It was proposed that the Mesoarchaeon (~3.3 Ga) was one of the major magmatic periods in the Nanling-Yunkai terrane of the West Cathaysia Block [4]. In addition, the Mesoarchaeon magmatic event was both involved in the juvenile input and the reworking of older crustal materials [4]. A previous study by Wang et al. (2018) [82] also reported a Paleoproterozoic detrital zircon grain of 3534 Ma with an  $\epsilon_{\text{Hf}}(t)$  value of 0.54 and Hf model age of 3774 Ma, demonstrating that juvenile materials should be involved in the formation of the Paleoproterozoic crust. In this work, a zircon grain from the Dengfuxian granites (#25) has a  $^{207}\text{Pb}/^{206}\text{Pb}$  age of 3252 Ma with a positive  $\epsilon_{\text{Hf}}(t)$  value of 3.7 and a Hf model age of 3357 Ma, which is similar to the zircon grain from the Tanghu granites (#3–13) with a  $^{207}\text{Pb}/^{206}\text{Pb}$  age of 3395 Ma,  $\epsilon_{\text{Hf}}(t)$  value of 3.09 and Hf model age of 3505 Ma. These data were nearly plotted along the evolutionary line of the depleted mantle in the age vs.  $\epsilon_{\text{Hf}}(t)$  diagram (Figure 9). Additionally, the crustal incubation time for these zircon grains is within the range of 150 Ma, indicating a juvenile crustal growth event (Figure 11). In conclusion, juvenile crustal growth might be predominant in the Archean for the West Cathaysia Block, however, limited crustal reworking events occurred in the Neo- and Meso-Archean.

#### 5.1.2. Paleoproterozoic (2500–1600 Ma)

It is well accepted that the 1.8–1.9 Ga magmatism is related to the assembly of the Columbia supercontinent [10,86,87]. Based on these exposed 1.89–1.86 Ga S-type granitoids, 1.85–1.83 Ga A-type granites, and ~1.77 Ga amphibolites in the Cathaysia Block, it was regarded that these rock units recorded a complete geodynamic process from collisional orogeny to intracontinental rifting during the Late Paleoproterozoic time, coinciding with the timing of final assembly and initial rifting of the Columbia supercontinent [22]. However, it is noteworthy that these Paleoproterozoic rocks are mainly hosted in the Wuyishan region of the East Cathaysia Block. Unlike the East Cathaysia Block, rocks with Paleoproterozoic ages have not been identified in the West Cathaysia Block so far. In addition, rare detrital zircon grains with Paleoproterozoic ages were discovered in the metamorphic rocks and fluvial sediment [4,22,28,82]. A remarkable difference with the East Cathaysia Block is that the peak ages of 1.8–1.9 Ga are absent in the West Cathaysia Block (Figure 10). It was proposed that the Nanling-Yunkai terrane of the West Cathaysia Block and the Wuyishan terrane of the East Cathaysia Block were separated from each other before the Neoproterozoic and finally united during the Grenvillian orogeny [4]. Therefore, the West Cathaysia Block might be unaffected by the assembly of the Columbia supercontinent in the Paleoproterozoic. Additionally, the crust generation and reworking of the West Cathaysia Block in this period is likely stagnant, due to the lack of coeval igneous/magmatic activities.

#### 5.1.3. Mesoproterozoic–Neoproterozoic (1600–540 Ma)

A consensus is that the SCB became a part of the supercontinent Rodinia in the Neoproterozoic, caused by the amalgamation of the Yangtze and Cathaysia Blocks during the Sibao orogeny, however, the timing of this amalgamation and the paleo-position of the SCB in Rodinia are still hotly debated [10,12,15,20]. Previous studies have indicated that the Neoproterozoic is one of the important crust accretion periods for the Cathaysia Block since the Precambrian detrital zircon ages from several (meta)sedimentary samples and river sands yield significant peaks at ca. 1.0 Ga and 0.8 Ga [4,10,19,82]. At the same time, these peak ages are consistent with the formation of igneous rocks of 1.0–0.9 Ga and 0.8–0.7 Ga, respectively [4,85,88–90]. As shown in Figure 10, zircon ages in the West and East Cathaysia Block both yield the two peaks at ca. 0.9–1.0 Ga and 0.8–0.9 Ga, respectively. The age spectrum of the West Cathaysia Block hosts a major peak at 0.9–1.0 Ga and a subordinate peak at 0.8–0.9 Ga, whereas the East Cathaysia Block shows the opposite data (Figure 10). This phenomenon might record the subducted–collisional process between the Yangtze and Cathaysia Blocks from northwest to southeast since the Wuyi-Yunkai arc-back-arc system

was proposed to be finally closed at ~920 Ma in the West Cathaysia Block, which was earlier than the closure age of 830–820 Ma for the Shuangxiwu arc or back-arc system in the Jiangnan Orogen Belt [89,91–94]. The Hf isotopes of these Neoproterozoic zircons contain both positive and negative  $\varepsilon_{\text{Hf}}(t)$  values, indicating that ancient and/or juvenile materials might be involved (Figure 9). However, the vast majority of corresponding Hf models' ages for these zircons are significantly older than the U-Pb ages, resulting in high values of crust incubation time (Figure 11). Consequently, it is inferred that the reworking of the juvenile and ancient crust might be predominant in the Mesoproterozoic–Neoproterozoic for the West Cathaysia Block.

### 5.2. Implications for the Regional Tungsten Mineralization

Tungsten is one of the strongly incompatible lithophile elements and tends to be enriched in crustal rocks. Therefore, the melting of abundant crustal rocks is necessary to form economically significant tungsten deposits [95–97]. In most cases, the formation of these tungsten deposits is commonly related to the granitic rocks which were involved in the ancient crustal materials, since tungsten has a high solubility in silicate melts [18,96,98,99]. In addition, tungsten becomes enriched in the late stage of these melts through intense fractional crystallization, supported by the fact that tungsten mineralization is commonly hosted in these highly fractionated granites [17,34,100–102]. However, tungsten mineralization is not exclusive to these highly fractionated melts. Lowly differentiated melts can also generate the formation of tungsten deposits, if the source of these melts is particularly rich in tungsten [96]. As discussed above, the crust evolution of the West Cathaysia Block is dominated by crustal reworking since the Proterozoic. Therefore, the long-term crustal reworking of the West Cathaysia Block enhances the enrichment of the economically valuable lithophile elements (e.g., W, Sn, U, Nb, and Ta) in the crust of the West Cathaysia Block.

The large-scale tungsten mineralization in the Nanling Range, explosively occurring in the Middle to Late Jurassic, was caused by the coeval granitic magmatism [103–106]. The formation of these granites and tungsten deposits in the Nanling Range is one of the hot issues in the last three decades, reaching a consensus that these granites are mostly highly fractionated granites and generated by the partial melting of the Cambrian basement rocks [17]. The Dengfuxian Jurassic granites related to the large-scale Xiangdong tungsten deposit host a series of ancient zircons which are mainly Proterozoic to Archean, indicating that complicated ancient sources were involved in the formation of the Dengfuxian Jurassic granites. In addition, almost all the Jurassic zircons have negative  $\varepsilon_{\text{Hf}}(t)$  values and old Hf model ages, suggesting that the Dengfuxian Jurassic granites were likely derived from the Proterozoic basement rocks of the West Cathaysia Block. In addition, this property is one of the favorable factors for the generation of economically valuable metal-enriched magma and related deposits.

## 6. Conclusions

Inherited zircons from the Mesozoic Dengfuxian and Paleozoic Tanghu plutons, the Nanling Range of the West Cathaysia Block, have U-Pb ages from the Neoproterozoic to the Archean. Together with the previously reported data, we conclude as follows: (1) The Hadean crust fragment might exist in the West Cathaysia Block and might have experienced the reworking event since at least 4100 Ma; (2) Archean zircons mainly originated from the depleted mantle and the juvenile crust generation was predominant in the Archean for the West Cathaysia Block; (3) The Proterozoic zircons mostly originated from the crustal source, and the crust evolution of the West Cathaysia Block has been dominated by the crust reworking since the Proterozoic. The Jurassic granites in the Nanling Range, formed by the partial melting of these Proterozoic rocks, are enriched in the metalliferous lithophile elements W, Sn, U, and Nb, causing the intense regional tungsten polymetallic mineralization.

**Supplementary Materials:** The following supporting information can be downloaded at: <https://www.mdpi.com/article/10.3390/min13040550/s1>, Table S1: LA-ICP-MS zircon U–Pb ages of the zircons from the Dengfuxian and Tanghu granites; Table S2: LA-MCICP-MS zircon Lu–Hf isotopes of the zircons from the Dengfuxian and Tanghu granites.

**Author Contributions:** J.C., Y.L. and L.L. conceived and designed the experiments; J.F., S.Y. and Q.W. took part in the discussion; G.X., X.Q. and Z.Z. took part in the field campaigns; J.C., Y.L. and L.L. wrote the paper. All authors have read and agreed to the published version of the manuscript.

**Funding:** This work was financially supported by the Open Fund of the Research Center for Petrogenesis and Mineralization of Granitoid Rocks, China Geological Survey (Nos. PM202308 and PMGR202008), China Postdoctoral Science Foundation (Grant No. 2022M710876), and the PI Project of Southern Marine Science and Engineering Guangdong Laboratory (Guangzhou) (Grant No. GML2020GD0802).

**Institutional Review Board Statement:** Not applicable.

**Informed Consent Statement:** Not applicable.

**Data Availability Statement:** Not applicable.

**Acknowledgments:** We appreciate the valuable and insightful suggestions and comments from the anonymous reviewers. We also thank the Ding He from the Department of Ocean Science of the Hong Kong University of Science & Technology for this excellent English editing work. We also thank Meirong Zheng for her kind support.

**Conflicts of Interest:** The authors declare no conflict of interest.

## References

- Thieblemont, D.; Delor, C.; Cocherie, A.; Lafon, J.M.; Goujou, J.C.; Balde, A.; Bah, M.; Sane, H.; Fanning, C.M. A 3.5 Ga granite–gneiss basement in Guinea: Further evidence for early Archean accretion within the West African Craton. *Precambrian Res.* **2001**, *108*, 179–194. [\[CrossRef\]](#)
- Marschik, R.; Mathur, R.; Ruiz, J.; Leveille, R.; de Almeida, A.J. Late Archean Cu–Au–Mo mineralization at Gameleira and Serra Verde, Carajas mineral Province, Brazil: Constraints from Re–Os molybdenite ages. *Miner. Depos.* **2005**, *39*, 983–991. [\[CrossRef\]](#)
- Zheng, Y.F.; Zhang, S.B. Formation and evolution of Precambrian continental crust in South China. *Chin. Sci. Bull.* **2007**, *52*, 1–12. (In Chinese with English Abstract) [\[CrossRef\]](#)
- Yu, J.H.; O'Reilly, Y.S.; Wang, L.J.; Griffin, W.L.; Zhou, M.F.; Zhang, M.; Shu, L.S. Components and episodic growth of Precambrian crust in the Cathaysia Block, South China: Evidence from U–Pb ages and Hf isotopes of zircons in Neoproterozoic sediments. *Precambrian Res.* **2010**, *181*, 97–114. [\[CrossRef\]](#)
- Payne, J.L.; Hand, M.; Pearson, N.J.; Barovich, K.M.; McInerney, D.J. Crustal thickening and clay: Controls on O isotope variation in global magmatism and siliciclastic sedimentary rocks. *Earth Planet. Sci. Lett.* **2015**, *412*, 70–76. [\[CrossRef\]](#)
- Tang, M.; Chen, K.; Rudnick, R.L. Archean upper crust transition from mafic to felsic marks the onset of plate tectonics. *Science* **2016**, *351*, 372–375. [\[CrossRef\]](#)
- Bucholz, C.E.; Biasi, J.A.; Beaudry, P.; Ono, S. Sulfur isotope behavior during metamorphism and anatexis of Archean sedimentary rocks: A case study from the Ghost Lake batholith, Ontario, Canada. *Earth Planet. Sci. Lett.* **2020**, *549*, 116494. [\[CrossRef\]](#)
- Li, R.Y.; Ke, S.; Li, S.G.; Song, S.G.; Wang, C. Origins of two types of Archean potassic granite constrained by Mg isotopes and statistical geochemistry: Implications for continental crustal evolution. *Lithos* **2020**, *368*, 105570. [\[CrossRef\]](#)
- Xu, X.S.; O'Reilly, Y.S.; Griffin, W.L.; Deng, P.; Pearson, N.J. Relict proterozoic basement in the Nanling Mountains (SE China) and its tectonothermal overprinting. *Tectonics* **2005**, *24*, 1–16. [\[CrossRef\]](#)
- Li, X.H.; Li, Z.X.; Li, W.X. Detrital zircon U–Pb age and Hf isotope constrains on the generation and reworking of Precambrian continental crust in the Cathaysia Block, South China: A synthesis. *Gondwana Res.* **2014**, *25*, 1202–1215. [\[CrossRef\]](#)
- Xu, X.; O'Reilly, S.Y.; Griffin, W.L.; Wang, X.; Pearson, N.J.; He, Z. The crust of Cathaysia: Age, assembly and reworking of two terranes. *Precambrian Res.* **2007**, *158*, 51–78. [\[CrossRef\]](#)
- Zhao, J.H.; Zhou, M.F.; Yan, D.P.; Zheng, J.P.; Li, J.W. Reappraisal of the ages of Neoproterozoic strata in South China: No connection with the Grenvillian orogeny. *Geology* **2011**, *39*, 299–302. [\[CrossRef\]](#)
- Li, X.H.; Li, Z.X.; He, B.; Li, W.X.; Li, Q.L.; Gao, Y.Y.; Wang, X.C. The Early Permian active continental margin and crustal growth of the Cathaysia Block: In situ U–Pb, Lu–Hf and O isotope analyses of detrital zircons. *Chem. Geol.* **2012**, *328*, 195–207. [\[CrossRef\]](#)
- Charvet, J. The Neoproterozoic–Early Paleozoic tectonic evolution of the South China Block: An overview. *J. Asian Earth Sci.* **2013**, *74*, 198–209. [\[CrossRef\]](#)
- Zhang, S.B.; Zheng, Y.F. Formation and evolution of Precambrian continental lithosphere in South China. *Gondwana Res.* **2013**, *23*, 1241–1260. [\[CrossRef\]](#)

16. Mao, J.R.; Li, Z.L.; Ye, H.M. Mesozoic tectono-magmatic activities in South China: Retrospect and prospect. *Sci. China–Earth Sci.* **2014**, *57*, 2853–2877. [[CrossRef](#)]
17. Cao, J.Y.; Yang, X.Y.; Du, J.G.; Wu, Q.H.; Kong, H.; Li, H.; Wan, Q.; Xi, X.S.; Gong, Y.S.; Zhao, H.R. Formation and geodynamic implication of the Early Yanshanian granites associated with W–Sn mineralization in the Nanling Range, South China: An overview. *Int. Geol. Rev.* **2018**, *60*, 1744–1771. [[CrossRef](#)]
18. Cao, J.Y.; Li, H.; Algeo, T.J.; Yang, L.; Tamehe, L.S. Two-stage magmatism and tungsten mineralization in the Nanling Range, South China: Evidence from the Jurassic Helukou deposit. *Am. Mineral.* **2021**, *106*, 1488–1502. [[CrossRef](#)]
19. Cawood, P.A.; Zhao, G.C.; Yao, J.L.; Wang, W.; Xu, Y.J.; Wang, Y.J. Reconstructing South China in Phanerozoic and Precambrian supercontinents. *Earth–Sci. Rev.* **2018**, *186*, 173–194. [[CrossRef](#)]
20. Yan, C.L.; Shu, L.S.; Faure, M.; Chen, Y.; Huang, R.B. Time constraints on the closure of the Paleo–South China Ocean and the Neoproterozoic assembly of the Yangtze and Cathaysia blocks: Insight from new detrital zircon analyses. *Gondwana Res.* **2019**, *73*, 175–189. [[CrossRef](#)]
21. Yu, J.H.; O'Reilly, Y.S.; Zhou, M.F.; Griffin, W.L.; Wang, L.J. U–Pb geochronology and Hf–Nd isotopic geochemistry of the Badu Complex, Southeastern China: Implications for the Precambrian crustal evolution and paleogeography of the Cathaysia Block. *Precambrian Res.* **2012**, *222*–223, 424–449. [[CrossRef](#)]
22. Yu, J.H.; Wang, L.J.; Griffin, W.L.; O'Reilly, S.Y.; Zhang, M.; Li, C.Z.; Shu, L.S. A Paleoproterozoic orogeny recorded in a long-lived cratonic remnant (Wuyishan terrane), eastern Cathaysia Block, China. *Precambrian Res.* **2009**, *174*, 347–363. [[CrossRef](#)]
23. Xia, Y.; Xu, X.S.; Zhu, K.Y. Paleoproterozoic S- and A-type granites in southwestern Zhejiang: Magmatism, metamorphism and implications for the crustal evolution of the Cathaysia basement. *Precambrian Res.* **2012**, *216*–219, 177–207. [[CrossRef](#)]
24. Zhao, L.; Zhou, X.W.; Zhai, M.G.; Santosh, M.; Geng, Y.S. Zircon U–Th–Pb–Hf isotopes of the basement rocks in northeastern Cathaysia block, South China: Implications for Phanerozoic multiple metamorphic reworking of a Paleoproterozoic terrane. *Gondwana Res.* **2015**, *28*, 246–261. [[CrossRef](#)]
25. Yu, J.H.; Zhang, C.H.; O'Reilly, Y.S.; Griffin, W.L.; Ling, H.F.; Sun, T.; Zhou, X.Y. Basement components of the Xiangshan–Yuhashan area, South China: Defining the boundary between the Yangtze and Cathaysia blocks. *Precambrian Res.* **2018**, *309*, 102–122. [[CrossRef](#)]
26. Xu, Y.J.; Du, Y.S.; Huang, H.W.; Huang, Z.Q.; Hu, L.S.; Zhu, Y.H.; Yu, W.C. Detrital zircon of 4.1 Ga in South China. *China Sci. Bull.* **2012**, *57*, 4356–4362. [[CrossRef](#)]
27. Xing, G.F.; Wang, X.L.; Wan, Y.S.; Chen, Z.H.; Jiang, Y.; Kitajima, L.; Ushikubo, T.; Gppon, P. Diversity in early crustal evolution: 4100 Ma zircons in the Cathaysia Block of southern China. *Sci. Rep.* **2014**, *4*, 5134. [[CrossRef](#)]
28. Li, X.Y.; Zhang, J.P.; Xiong, Q.; Zhou, X.; Lu, X. Triassic rejuvenation of unexposed Archean–Paleoproterozoic deep crust beneath the western Cathaysia block, South China. *Tectonophysics* **2018**, *724*–725, 65–79. [[CrossRef](#)]
29. Xiong, C.; Chen, H.D.; Niu, Y.L.; Chen, A.Q.; Zhang, C.G.; Li, F.; Xu, S.L.; Yang, S. Provenance, depositional setting, and crustal evolution of the Cathaysia Block, South China: Insights from detrital zircon U–Pb geochronology and geochemistry of clastic rocks. *Geol. J.* **2019**, *54*, 897–912. [[CrossRef](#)]
30. Zheng, J.P.; Griffin, W.L.; Tang, H.Y.; Zhang, Z.H.; Su, Y.P.; Liu, G.L. Archean basement similar to the North China and Yangtze continents may be existed beneath the western Cathaysia. *Geol. J. China Univ.* **2008**, *14*, 549–557. (In Chinese with English Abstract)
31. Yang, Z.Y.; Jiang, S.Y. Detrital zircons in metasedimentary rocks of Mayuan and Mamianshan Group from Cathaysia Block in northwestern Fujian Province, South China: New constraints on their formation ages and paleogeographic implication. *Precambrian Res.* **2019**, *320*, 13–30. [[CrossRef](#)]
32. Brown, M. Crustal melting and granite magmatism: Key issues. *Phys. Chem. Earth Part A Solid Earth Geod.* **2001**, *26*, 201–212. [[CrossRef](#)]
33. Lopez, S.; Fernandez, C.; Castro, A. Evolution of the Archaean continental crust: Insights from the experimental study of Archaean granitoids. *Curr. Sci.* **2006**, *91*, 607–621.
34. Wu, F.Y.; Liu, X.C.; Ji, W.Q.; Wang, J.M.; Yang, L. Highly fractionated granites: Recognition and research. *Sci. China–Earth Sci.* **2017**, *60*, 1201–1219. [[CrossRef](#)]
35. Ni, P.; Wang, G.G.; Li, W.S.; Chi, Z.; Li, S.N.; Gao, Y. A review of the Yanshanian ore-related felsic magmatism and tectonic settings in the Nanling W–Sn and Wuyi Au–Cu metallogenic belts, Cathaysia Block, South China. *Ore Geol. Rev.* **2021**, *133*, 104088. [[CrossRef](#)]
36. Pidgeon, R.T.; Bosch, D.; Bruguier, O. Inherited zircon and titanite U–Pb systems in an archaean syenite from southwestern Australia: Implications for U–Pb stability of titanite. *Earth Planet. Sci. Lett.* **1996**, *141*, 187–198. [[CrossRef](#)]
37. Zeck, H.P.; Wingate, M.T.D.; Pooley, G.D.; Ugidis, J.M. A sequence of Pan–African and Hercynian events recorded in zircons from an orthogneiss from the Hercynian belt of western central Iberia —An ion microprobe U–Pb study. *J. Petrol.* **2004**, *45*, 1613–1629. [[CrossRef](#)]
38. Flowerdew, M.J.; Millar, I.L.; Vaughan, A.P.M.; Horstwood, M.S.A.; Fanning, C.M. The source of granitic gneisses and migmatites in the Antarctic Peninsula: A combined U–Pb SHRIMP and laser ablation Hf isotope study of complex zircons. *Contrib. Mineral. Petrol.* **2006**, *151*, 751–768. [[CrossRef](#)]

39. Qiao, L.; Wang, Q.F.; Li, C.S. The western segment of the suture between the Yangtze and Cathaysia blocks: Constraints from inherited and co-magmatic zircons from Permian S-type granitoids in Guangxi, South China. *Terra Nova* **2015**, *27*, 392–398. [\[CrossRef\]](#)
40. Gao, S.; Ling, W.L.; Qiu, Y.M.; Liang, Z.; Hartmann, G.; Simon, K. Contrasting geochemical and Sm–Nd isotopic compositions of Archean metasediments from the Kongling high-grade terrain of the Yangtze craton: Evidence for cratonic evolution and redistribution of REE during crustal anatexis. *Geochim. Et Cosmochim. Acta* **1999**, *63*, 2071–2088. [\[CrossRef\]](#)
41. Gao, S.; Yang, J.; Zhou, L.; Li, M.; Hu, Z.C.; Guo, J.L.; Yuan, H.L.; Gong, H.J.; Xiao, G.Q.; Wei, J.Q. Age and growth of the Archean Kongling terrain, South China, with emphasis on 3.3 Ga granitoid gneisses. *Am. J. Sci.* **2011**, *311*, 153–182. [\[CrossRef\]](#)
42. Zhang, S.B.; Zheng, Y.F.; Wu, Y.B.; Zhao, Z.F.; Gao, S.; Wu, F.Y. Zircon isotope evidence for  $\geq 3.5$  Ga continental crust in the Yangtze craton of China. *Precambrian Res.* **2006**, *146*, 16–34. [\[CrossRef\]](#)
43. Jiao, W.F.; Wu, Y.B.; Yang, S.H.; Peng, M.; Wang, J. The oldest basement rock in the Yangtze Craton revealed by zircon U–Pb age and Hf isotope composition. *Sci. China Ser. D Earth Sci.* **2009**, *52*, 1393–1399. [\[CrossRef\]](#)
44. Chen, K.; Gao, S.; Wu, Y.B.; Guo, J.L.; Hu, Z.C.; Liu, Y.S.; Zong, K.Q.; Liang, Z.W.; Geng, X.L. 2.6–2.7 Ga crustal growth in Yangtze craton, South China. *Precambrian Res.* **2013**, *224*, 472–490. [\[CrossRef\]](#)
45. Cui, X.Z.; Wang, J.; Wang, X.C.; Wilde, S.A.; Ren, G.M.; Li, S.J.; Deng, Q.; Ren, F.; Liu, J.P. Early crustal evolution of the Yangtze Block: Constraints from zircon U–Pb–Hf isotope systematics of 3.1–1.9 Ga granitoids in the Cuoke Complex, SW China. *Precambrian Res.* **2021**, *357*, 106155. [\[CrossRef\]](#)
46. Zhang, Y.Z.; Wang, Y.J.; Geng, H.Y.; Zhang, Y.H.; Fan, W.M.; Zhong, H. Early Neoproterozoic (similar to 850 Ma) back-arc basin in the Central Jiangnan Orogen (Eastern South China): Geochronological and petrogenetic constraints from meta-basalts. *Precambrian Res.* **2013**, *231*, 325–342. [\[CrossRef\]](#)
47. Yao, J.L.; Shu, L.S.; Santosh, M.; Zhao, G.C. Neoproterozoic arc-related mafic–ultramafic rocks and syn-collision granite from the western segment of the Jiangnan Orogen, South China: Constraints on the Neoproterozoic assembly of the Yangtze and Cathaysia Blocks. *Precambrian Res.* **2014**, *243*, 39–62. [\[CrossRef\]](#)
48. Deng, T.; Xu, D.R.; Chi, G.X.; Zhu, Y.H.; Wang, Z.L.; Chen, G.W.; Li, Z.H.; Zhang, J.L.; Ye, T.W.; Yu, D.S. Revisiting the ca. 845–820–Ma S-type granitic magmatism in the Jiangnan Orogen: New insights on the Neoproterozoic tectono-magmatic evolution of South China. *Int. Geol. Rev.* **2019**, *61*, 383–403. (In Chinese with English Abstract) [\[CrossRef\]](#)
49. Wan, L.; Kusky, T.M.; Jin, W.; Yang, J.; Zeng, Z.X. Neoproterozoic tectonics of the Jiangnan orogen: The magmatic record of continental growth by arc and slab-failure magmatism from 1000 to 780 Ma. *Precambrian Res.* **2021**, *362*, 106319.
50. Li, X.H. U–Pb zircon ages of granites from the southern margin of the Yangtze Block: Timing of Neoproterozoic Jinning: Orogeny in SE China and implications for Rodinia Assembly. *Precambrian Res.* **1999**, *97*, 43–57. [\[CrossRef\]](#)
51. Wang, R.R.; Xu, Z.Q.; Santosh, M.; Zeng, B. Mid-Neoproterozoic magmatism in the northern margin of the Yangtze Block, South China: Implications for transition from subduction to post-collision. *Precambrian Res.* **2021**, *354*, 106073. [\[CrossRef\]](#)
52. Xie, J.C.; Yang, X.Y.; Sun, W.D.; Du, J.G. Early Cretaceous dioritic rocks in the Tongling region, eastern China: Implications for the tectonic settings. *Lithos* **2012**, *150*, 49–61. [\[CrossRef\]](#)
53. Mao, Z.H.; Liu, J.J.; Mao, J.W.; Deng, J.; Zhang, F.; Meng, X.Y.; Xiong, B.K.; Xiang, X.K.; Luo, X.H. Geochronology and geochemistry of granitoids related to the giant Dahutang tungsten deposit, middle Yangtze River region, China: Implications for petrogenesis, geodynamic setting, and mineralization. *Gondwana Res.* **2015**, *28*, 816–836. [\[CrossRef\]](#)
54. Zhou, T.F.; Wang, S.W.; Fan, Y.; Yuan, F.; Zhang, D.Y.; White, N.C. A review of the intracontinental porphyry deposits in the Middle–Lower Yangtze River Valley metallogenic belt, Eastern China. *Ore Geol. Rev.* **2015**, *65*, 433–456. [\[CrossRef\]](#)
55. Song, S.W.; Mao, J.W.; Xie, G.Q.; Lehmann, B.; Jian, W.; Wang, X.G. The world-class mid-Mesozoic Jiangnan tungsten belt, South China: Coeval large reduced and small oxidized tungsten systems controlled by different magmatic petrogenesis. *Ore Geol. Rev.* **2021**, *139*, 104543. [\[CrossRef\]](#)
56. Xiao, Q.L.; Zhou, T.F.; Holling, P.; Wang, S.W.; Liu, J.; Yang, Q.G.; Yuan, F. Mineral and whole-rock chemistry of the Chating porphyry Cu–Au deposit related intrusions in the Middle–Lower Yangtze River Belt, Eastern China: Implications for magma evolution and mineralization. *Lithos* **2021**, *380*, 105881. [\[CrossRef\]](#)
57. Cao, J.Y.; Li, H.; Yang, X.Y.; Tamehe, L.S.; Esmaeili, R. Multi-stage magma evolution recorded by apatite and zircon of adakite-like rocks: A case study from the Shatanjiao intrusion, Tongling region, Eastern China. *Am. Mineral.* **2022**, *107*, 178–189. [\[CrossRef\]](#)
58. Zhou, X.M.; Sun, T.; Shen, W.Z.; Shu, L.S.; Niu, Y.L. Petrogenesis of Mesozoic granitoids and volcanic rocks in South China: A response to tectonic evolution. *Episodes* **2006**, *29*, 26–33. [\[CrossRef\]](#) [\[PubMed\]](#)
59. Hu, X.J.; Xu, J.K.; Tong, Z.X.; Chen, C.H. *The Precambrian Geology of Southwestern Zhejiang Province*; Geological Publishing House: Beijing, China, 1991; pp. 1–278. (In Chinese with English Abstract)
60. Hu, X.J.; Xu, J.K.; Tong, Z.X.; Chen, C.H. Geochronology of the Middle Proterozoic Longquan Group in Southwestern Zhejiang. *Geol. Rev.* **1992**, *38*, 271–278. (In Chinese with English Abstract)
61. Wang, W.; Zhou, M.F.; Yan, D.P.; Li, J.W. Depositional age, provenance, and tectonic setting of the Neoproterozoic Sibao group, Southeastern Yangtze Block, South China. *Precambrian Res.* **2012**, *192–195*, 107–124. [\[CrossRef\]](#)
62. Guo, C.L.; Liu, Z.K. Caledonian granites in South China: The geological and geochemical characteristics on their petrogenesis and mineralization. *J. Earth Sci. Environ.* **2021**, *43*, 927–961. (In Chinese with English Abstract)

63. Cai, Y.; Lu, J.J.; Ma, D.S.; Huang, H.; Zhang, H.F. Chronology and geochemical characteristics of Late Indosinian Dengfuxian two-mica granite in eastern Hunan Province, China, and its significance. *Acta Petrol. Sin.* **2013**, *29*, 4215–4231. (In Chinese with English Abstract)
64. He, M.; Liu, Q.; Hou, Q.L.; Sun, J.F.; Zhang, J.H.; Wu, S.C.; Zhu, H.F. Petrogenesis of the Dengfuxian granite, eastern Hunan Province and constraints on mineralization: Evidences from zircon and cassiterite U–Pb geochronology, zircon Hf–O isotopes and whole-rock geochemistry. *Acta Petrol. Sin.* **2018**, *34*, 637–655.
65. Li, H.; Cao, J.Y.; Algeo, T.J.; Jiang, W.C.; Liu, B.; Wu, Q.H. Zircons reveal multi-stage genesis of the Xiangdong (Dengfuxian) tungsten deposit, South China. *Ore Geol. Rev.* **2019**, *111*, 102979. [\[CrossRef\]](#)
66. Cao, J.Y.; Wu, Q.H.; Yang, X.Y.; Deng, X.T.; Li, H.; Kong, H.; Xi, X.S. Geochemical factors revealing the differences between the Xitian and Dengfuxian composite plutons, middle Qin–Hang Belt: Implications to the W–Sn mineralization. *Ore Geol. Rev.* **2020**, *118*, 103353. [\[CrossRef\]](#)
67. Deng, X.T.; Cao, J.Y.; Wu, Q.H.; Kong, H.; Xi, X.S. Difference of sources of the Yanshanian Xitian and Dengfuxian granites in Hunan Province and their implication. *J. Cent. South Univ. Sci. Technol.* **2017**, *48*, 212–222.
68. Xia, J.L.; Huang, G.C.; Ding, L.; Ding, L.X.; Chen, X.Q.; Ji, W.B. Chronological Framework of the Zhuguangshan Composite Batholith in the Nanling Area. *South China Geol.* **2021**, *37*, 280–297. (In Chinese with English Abstract)
69. Wiedenbeck, M.; Alle, P.; Corfu, F.; Griffin, W.L.; Meier, M.; Ober, F.; Von Quadt, A.; Roddick, J.C.; Spiegel, W. Three natural zircon standards for U–Th–Pb, Lu–Hf, trace-element and REE analyses. *Geostand. Newsl.* **1995**, *19*, 1–23. [\[CrossRef\]](#)
70. Andersen, T. Correction of common lead in U–Pb analyses that do not report 204Pb. *Chem. Geol.* **2002**, *192*, 59–79. [\[CrossRef\]](#)
71. Liu, Y.; Gao, S.; Hu, Z.; Gao, C.; Zong, K.; Wang, D. Continental and oceanic crust recycling-induced melt–peridotite interactions in the trans–north china orogen: U–Pb dating, Hf isotopes and trace elements in zircons from mantle xenoliths. *J. Petrol.* **2010**, *51*, 537–571. [\[CrossRef\]](#)
72. Ludwig, K.R. *ISOPLOT 3.00: A Geochronological Toolkit for Microsoft Excel*; Berkeley Geochronology Center: Berkeley, CA, USA, 2003; p. 39.
73. Thirlwall, M.F.; Anczkiewicz, R. Multidynamic isotope ratio analysis using MC–ICP–MS and the causes of secular drift in Hf, Nd and Pb isotope ratios. *Int. J. Mass Spectrom.* **2004**, *235*, 59–81. [\[CrossRef\]](#)
74. Blichert-Toft, J.; Chauvel, C.; Albarède, F. Separation of Hf and Lu for high-precision isotope analysis of rock samples by magnetic sector–multiple collector ICP–MS. *Contrib. Mineral. Petrol.* **1997**, *127*, 248–260. [\[CrossRef\]](#)
75. Wu, F.; Yang, Y.; Xie, L.; Yang, J.; Xu, P. Hf isotopic compositions of the standard zircons and baddeleyites used in U–Pb geochronology. *Chem. Geol.* **2006**, *234*, 105–126. [\[CrossRef\]](#)
76. Sláma, J.; Košler, J.; Condon, D.J.; Crowley, J.L.; Gerdes, A.; Hanchar, J.M.; Horstwood, M.S.A.; Morris, G.A.; Nasdala, L.; Norberg, N.; et al. Plešovice zircon—A new natural reference material for U–Pb and Hf isotopic microanalysis. *Chem. Geol.* **2008**, *249*, 1–35. [\[CrossRef\]](#)
77. Söderlund, U.; Patchett, P.J.; Vervoort, J.D.; Isachsen, C.E. The <sup>176</sup>Lu decay constant determined by Lu–Hf and U–Pb isotope systematics of Precambrian mafic intrusions. *Earth Planet. Sci. Lett.* **2004**, *219*, 311–324. [\[CrossRef\]](#)
78. Bouvier, A.; Vervoort, J.D.; Patchett, P.J. The Lu–Hf and Sm–Nd isotopic composition of CHUR: Constraints from unequilibrated chondrites and implications for the bulk composition of terrestrial planets. *Earth Planet. Sci. Lett.* **2008**, *273*, 48–57. [\[CrossRef\]](#)
79. Griffin, W.L.; Wang, X.; Jackson, S.E.; Pearson, N.J.; O'Reilly, S.Y.; Xu, X.; Zhou, X. Zircon chemistry and magma mixing, SE China: In-situ analysis of Hf isotopes, Tonglu and Pingtan igneous complexes. *Lithos* **2002**, *61*, 237–269. [\[CrossRef\]](#)
80. Hoskin, P.W.O.; Schaltegger, U. The composition of zircon and igneous and metamorphic petrogenesis. *Rev. Mineral. Geochem.* **2003**, *53*, 27–62. [\[CrossRef\]](#)
81. Li, X.C.; Wang, A.D.; Wan, J.J.; Lin, L.F. The ctustal growth and evolution of Cathaysia block: Constraints from detrital zircon Lu–Hf isotopes of the ganjiang river sediments. *Sci. Technol. Eng.* **2017**, *17*, 145–153.
82. Wang, K.X.; Sun, L.Q.; Sun, T.; Huang, H.; Qin, L.S. Provenance, weathering conditions, and tectonic evolution history of the Cambrian meta-sediments in the Zhuguangshan area, Cathaysia Block. *Precambrian Res.* **2018**, *311*, 195–210.
83. Wang, C.Y.; Campbell, I.H.; Allen, C.M.; Williams, I.S.; Eggins, S.M. Rate of growth of the preserved North American continental crust: Evidence from Hf and O isotopes in Mississippi detrital zircons. *Geochim. Et Cosmochim. Acta* **2009**, *73*, 712–728. [\[CrossRef\]](#)
84. Wang, C.Y.; Campbell, I.H.; Stepanov, A.S.; Allen, C.M.; Burtsev, I.N. Growth rate of the preserved continental crust: II. Constraints from Hf and O isotopes in detrital zircons from Greater russian rivers. *Geochim. Et Cosmochim. Acta* **2011**, *75*, 1308–1345. [\[CrossRef\]](#)
85. Zhang, A.M.; Wang, Y.J.; Fan, W.M.; Zhang, Y.Z.; Yang, J. Earliest Neoproterozoic (ca. 1.0 Ga) arc–back–arc basin nature along the northern Yunkai Domain of the Cathaysia Block: Geochronological and geochemical evidence from the metabasite. *Precambrian Res.* **2012**, *220–221*, 217–233. [\[CrossRef\]](#)
86. Meert, J.G.; Santosh, M. The Columbia supercontinent revisited. *Gondwana Res.* **2017**, *50*, 67–83. [\[CrossRef\]](#)
87. Chaves, A.D. Columbia (Nuna) supercontinent with external subduction girdle and concentric accretionary, collisional and intracontinental orogens permeated by large igneous provinces and rifts. *Precambrian Res.* **2021**, *352*, 106017. [\[CrossRef\]](#)
88. Shu, L.S.; Faure, M.; Yu, J.H.; Jahn, B.M. Geochronological and geochemical features of the Cathaysia block (South China): New evidence for the Neoproterozoic breakup of Rodinia. *Precambrian Res.* **2011**, *187*, 263–276. [\[CrossRef\]](#)
89. Wang, Y.J.; Zhang, Y.Z.; Fan, W.M.; Geng, H.Y.; Zou, H.P.; Bi, X.W. Early Neoproterozoic accretionary assemblage in the Cathaysia Block: Geochronological, Lu–Hf isotopic and geochemical evidence from granitoid gneisses. *Precambrian Res.* **2014**, *249*, 144–161. [\[CrossRef\]](#)

90. Sun, J.J.; Shu, L.S.; Santosh, M.; Wang, L.S. Precambrian crustal evolution of the central Jiangnan Orogen (South China): Evidence from detrital zircon U–Pb ages and Hf isotopic compositions of Neoproterozoic metasedimentary rocks. *Precambrian Res.* **2018**, *318*, 1–24. [\[CrossRef\]](#)
91. Li, W.X.; Li, X.H.; Li, Z.X. Neoproterozoic bimodal magmatism in the Cathaysia Block of South China and its tectonic significance. *Precambrian Res.* **2005**, *136*, 51–66. [\[CrossRef\]](#)
92. Li, W.X.; Li, X.H.; Li, Z.X. Ca. 850 Ma bimodal volcanic rocks in northeastern Jiangxi South China: Initial extension during the breakup of Rodinia. *Am. J. Sci.* **2010**, *310*, 951–980. [\[CrossRef\]](#)
93. Wang, Y.J.; Fan, W.M.; Zhang, G.W.; Zhang, Y.H. Phanerozoic tectonics of the South China Block: Key observations and controversies. *Gondwana Res.* **2013**, *23*, 1273–1305. [\[CrossRef\]](#)
94. Wang, Y.J.; Zhang, A.M.; Cawood, P.A.; Fan, W.M.; Xu, J.F.; Zhang, G.W.; Zhang, Y.Z. Geochronological, geochemical and Nd–Hf–Os isotopic fingerprinting of an early Neoproterozoic arc–back–arc system in South China and its accretionary assembly along the margin of Rodinia. *Precambrian Res.* **2013**, *231*, 343–371. [\[CrossRef\]](#)
95. Rasmussen, K.L.; Lentz, D.R.; Falck, H.; Pattison, D.R.M. Felsic magmatic phases and the role of late–stage aplitic dykes in the formation of the world–class Cantung Tungsten skarn deposit, Northwest Territories, Canada. *Ore Geol. Rev.* **2011**, *41*, 75–111. [\[CrossRef\]](#)
96. Romer, R.L.; Kroner, U. Phanerozoic tin and tungsten mineralization–Tectonic controls on the distribution of enriched protoliths and heat sources for crustal melting. *Gondwana Res.* **2016**, *31*, 60–95. [\[CrossRef\]](#)
97. Korges, M.; Weis, P.; Lueders, V.; Laurent, O. Depressurization and boiling of a single magmatic fluid as a mechanism for tin–tungsten deposit formation. *Geology* **2018**, *46*, 75–78. [\[CrossRef\]](#)
98. Walter, M.J.; Thibault, T. Partitioning of tungsten and molybdenum between metallic liquid and silicate melt. *Science* **1995**, *270*, 1186–1189. [\[CrossRef\]](#)
99. Schmidt, C.; Romer, R.L.; Wohlgemuth–Ueberwasser, C.C.; Appelt, O. Partitioning of Sn and W between granitic melt and aqueous fluid. *Ore Geol. Rev.* **2020**, *117*, 103261. [\[CrossRef\]](#)
100. Shu, X.J.; Wang, X.L.; Sun, T.; Xu, X.S.; Dai, M.N. Trace elements, U–Pb ages and Hf isotopes of zircons from Mesozoic granites in the western Nanling Range, South China: Implications for petrogenesis and W–Sn mineralization. *Lithos* **2011**, *127*, 468–482. [\[CrossRef\]](#)
101. Guo, C.L.; Chen, Y.C.; Zeng, Z.L.; Lou, F.S. Petrogenesis of the Xihuashan granites in southeastern China: Constraints from geochemistry and in–situ analyses of zircon U–Pb–Hf–O isotopes. *Lithos* **2012**, *148*, 209–227. [\[CrossRef\]](#)
102. Chen, Y.; Li, H.; Sun, W.; Ireland, T.; Tian, X.; Hu, Y.; Yang, W.; Chen, C.; Xu, D. Generation of Late Mesozoic Qianlishan A2–type granite in Nanling Range, South China: Implications for Shizhuyuan W–Sn mineralization and tectonic evolution. *Lithos* **2016**, *266*, 435–452. [\[CrossRef\]](#)
103. Hua, R.M.; Chen, P.R.; Zhang, W.L.; Yao, J.M.; Lin, J.F.; Zhang, Z.S.; Gu, S.Y. Metallogenesis and their geodynamic settings related to Mesozoic granitoids in the Nanling Range. *Geol. J. China Univ.* **2005**, *11*, 291–304, (In Chinese with English Abstract).
104. Mao, J.W.; Cheng, Y.B.; Chen, M.H.; Pirajno, F. Major types and time–space distribution of Mesozoic ore deposits in South China and their geodynamic settings. *Miner. Depos.* **2013**, *48*, 267–294.
105. Mao, J.W.; Xie, G.Q.; Guo, C.L.; Chen, Y.C. Largescale tungsten–tin mineralization in the Nanling region, South China: Metallogenic ages and corresponding geodynamic processes. *Acta Petrol. Sin.* **2007**, *23*, 2329–2338. (In Chinese with English Abstract)
106. Chen, J.; Wang, R.C.; Zhu, J.C.; Lu, J.J.; Ma, D.S. Multiple–aged granitoids and related tungsten–tin mineralization in the Nanling Range, South China. *Sci. China Earth Sci.* **2013**, *56*, 2045–2055. [\[CrossRef\]](#)

**Disclaimer/Publisher’s Note:** The statements, opinions and data contained in all publications are solely those of the individual author(s) and contributor(s) and not of MDPI and/or the editor(s). MDPI and/or the editor(s) disclaim responsibility for any injury to people or property resulting from any ideas, methods, instructions or products referred to in the content.